Effects of multi-helicity confinement fields on zonal flows and ion temperature gradient turbulence

Tomo-Hiko WATANABE[1,2], Sergi FERRANDO-MARGALET[1], and Hideo SUGAMA[1,2]

[1]*National Institute for Fusion Science, Toki 509-5292, Japan*

[2]*The Graduate University for Advanced Studies (Sokendai), Toki 509-5292, Japan*

October 17, 2007

Effects of multi-helicity confinement magnetic fields on zonal flows and ion temperature gradient (ITG) turbulence are investigated by means of the gyrokinetic-Vlasov simulation code (GKV code). Detailed magnetic field parameters for the standard and inward-shifted configurations of the Large Helical Device (LHD) experiments are introduced in the simulation model. By the linear GKV simulations, it has been shown that, in the inward-shifted configuration, the maximum ITG mode growth rate slightly increases while the zonal flow is maintained for a longer time [S. Ferrando-Margalet, H. Sugama, and T.-H. Watanabe, "*Zonal flows and ion temperature gradient instabilities in multiple-helicity magnetic fields*" Phys. Plasmas (2007) in press]. Correspondingly, the nonlinear GKV simulations of the ITG turbulence in simple model configurations are extended to the more elaborate ones in the present study. The obtained results show effective regulation of the ITG turbulence by the zonal flows in the inward-shifted case. The zonal flows generated with three-times larger averaged amplitudes than those in the standard configuration lead to a lower ion heat transport level. The obtained results confirm the theoretical prediction that the neoclassical optimization of helical systems contributes to reduction of the anomalous transport by enhancing the zonal-flow level.

Keywords: zonal flow, ITG turbulence, gyrokinetic simulation, helical system, LHD

1 Introduction

Sheared $\boldsymbol{E} \times \boldsymbol{B}$ plasma flows with toroidal and poloidal symmetries, namely the zonal flows, have widely been believed as one of key ingredients for regulating the turbulent transport in magnetic confinement fusion [1]. In toroidal systems, the zonal flow is coupled to the geodesic acoustic mode (GAM) oscillation [2]. A linear response of the zonal flow driven by the ion temperature gradient (ITG) turbulence in a tokamak was derived from the gyrokinetic theory by Rosenbluth and Hinton [3]. It is considered that the residual zonal flow remaining constant after Landau damping of the GAM plays an important role in reduction of the tokamak ITG turbulent transport.

The gyrokinetic theory of the zonal flow has been extended to helical systems [4, 5], and the idea of the zonal flow optimization for effective reduction of the turbulent transport has come out [4, 5, 6]. The zonal flow was first identified in the Compact Helical System (CHS) experiments [7], and is recognized as a mutual important subject in the anomalous transport studies for tokamak and helical systems.

The role of zonal flows in regulating the turbulence is, thus, investigated for understanding the transport property observed in the Large Helical Device (LHD) [8] experiments. From the LHD experiments it is found that not only the neoclassical but also the anomalous transport is reduced in the inward-shifted configuration [9]. Here, it is noteworthy that the radial drift motion of helical-ripple-trapped particles is decreased by shifting the magnetic axis inward while the unfavorable magnetic curvature destabilizing the ballooning-type modes such as the toroidal ITG mode is increased. The gyrokinetic theory of zonal flows in helical systems has shown that the slower decay of the zonal flow expected in the inward-shifted LHD configuration lead to lower turbulent transport than that in the standard one [4, 5]. The theoretical estimate of the linear response of the zonal flow is verified by the gyrokinetic-Vlasov simulations [4, 5, 10, 11] by means of the GKV code [12]. The nonlinear GKV simulations for the simplified models of the LHD have demonstrated that the ITG turbulent transport in the inward-shifted configuration, which has 60% larger growth rates of the ITG stability, is regulated by the stronger zonal flows to a level comparable to the standard case [10].

In the present study, realistic parameter sets for the LHD experimental conditions are employed in the GKV simulations of the ITG turbulence, where differences in the linear stability between the standard and inward-shifted cases become smaller [11, 13] while slower decay of the zonal flow in the inward-shifted case. Then, it is expected that the lower anomalous transport will be found in the inward-shifted case, as actually observed in the LHD experiments. This paper is organized as follows. After a brief introduction of our simulation model in section 2, the GKV simulation results of the ITG turbulence and zonal flows are shown in section 3. A conclusion is given in section 4.

author's e-mail: watanabe.tomohiko@nifs.ac.jp

Table 1 Parameters used in GKV simulations of ITG turbulence and zonal flows in LHD model configurations.

	Standard	Inward-shifted
r/R_0	0.099	0.114
q_0	1.9	1.7
$\hat{s}$	-0.85	-0.96
ϵ_t	0.087	0.082
ϵ_L/ϵ_t	0.91	1.20
$\epsilon_{L-1}/\epsilon_t$	-0.28	-0.74
$\epsilon_{L+1}/\epsilon_t$	0	-0.24
$(r/\epsilon_t)\epsilon'_{00}$	0.22	0.71
$(r/\epsilon_t)\epsilon'_t$	1.02	1.00
$(r/\epsilon_t)\epsilon'_L$	1.96	2.44
$(r/\epsilon_t)\epsilon'_{L-1}$	-0.63	-0.36
$(r/\epsilon_t)\epsilon'_{L+1}$	0	-0.61

2 Simulation Model

The nonlinear gyrokinetic equation [14] for the perturbed ion gyrocenter distribution function, δf, in the low-β electrostatic limit is numerically solved by the GKV code [12] as a partial differential equation defined on the five-dimensional phase-space. We introduce a model collision term given by the gyrophase average of the Lenard-Bernstein collision operator [15]. The quasi-neutrality condition with the adiabatic electron response (for $T_e = T_i$) is used for calculation of the electrostatic potential, ϕ_{k_x,k_y}. In the GKV code, we employ the toroidal flux tube model [16] with the field-aligned coordinates, and also assume constant volume-averaged density and temperature gradients with scale-lengths of L_n and L_T as well as the constant magnetic shear parameter, $\hat{s} = (r_0/q_0)dq/dr$. Here, $q(r)$ stands for the safety factor, and $q_0 = q(r_0)$. See Ref. [12] for more details.

In the helical version of the GKV code, the averaged minor radius, r_0, is defined by $\Psi_t = \pi B_0 r_0^2$ where Ψ_t means the toroidal flux. The toroidal and helical effects of the confinement field are introduced by the change of magnetic field strength,

$$B = B_0 \left\{1 - \epsilon_{00}(r) - \epsilon_t(r)\cos z - \sum_{l=L-1}^{l=L+1} \epsilon_l(r)\cos[(l - Mq_0)z - M\alpha]\right\}, \quad (1)$$

where L and M denote the poloidal and toroidal periodicities of the main component of the helical field. For the LHD, $L = 2$ and $M = 10$. The main helical field is represented by ϵ_L. The side-band components and the averaged normal curvature are also given by ϵ_{L-1}, ϵ_{L+1}, and $\epsilon'_{00} = d\epsilon_{00}/dr$, respectively. We also set the field-line label α to be constant ($\alpha = 0$) because of weak α-dependence of the linear ITG instability. For the ITG turbulence simulations shown below, we employ a huge number of grid points over 50 billions [that is, $128 \times 128 \times 512 \times 128 \times 48$ in the fluxtube coordinates of $(x, y, z, v_\parallel, \mu)$ of the five-dimensional phase-space]. Further details of the GKV simulation model for helical systems are found in Ref. [10].

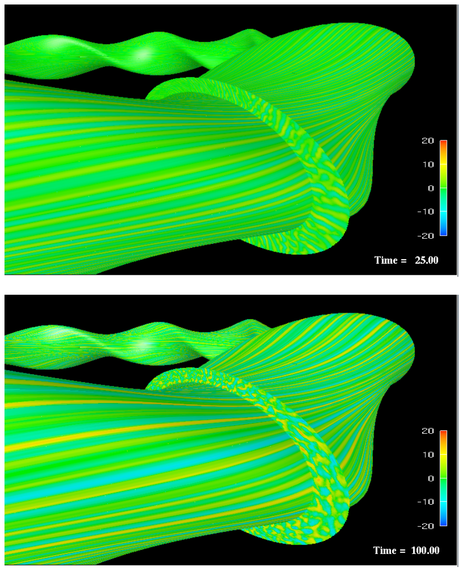

Fig. 1 Color contours of the electrostatic potential of the zonal flow and the ITG turbulence obtained by the GKV simulation for the standard model configurations at $t = 25$ (upper) and $t = 100L_n/v_{ti}$ (lower).

3 Gyrokinetic Simulation of ITG Turbulence and Zonal Flows

Nonlinear gyrokinetic simulations of the ITG turbulence and zonal flows for helical systems [10] are extended so as to incorporate the realistic parameter sets for the LHD experiments as has been done in the linear GKV simulations of the ITG instability and zonal flows [11]. Differences in the linear growth rates of the ITG instability between the standard and inward-shifted model configurations, which were about 60% in Ref. [10], are largely decreased by using the new parameter sets [11]. Moreover, the collisionless decay of the zonal flow in the realistic model for the inward-shifted configuration takes longer time than those for the standard and the previous cases [11]. These results support the scenario derived from the theoretical analysis of the zonal flow response in helical systems [4, 5], such that the stronger zonal flow driven by the ITG turbulence in the inward-shifted case may lead to a lower level of the turbulent transport than that in the standard configuration.

The GKV code employs the toroidal flux tube domain with the same local plasma parameters of $\eta_i \equiv L_n/L_{Ti} = 3$, $L_n/R_0 = 0.3$, $T_e/T_i = 1$, and $\alpha = 0$ for the standard and inward-shifted cases. Other parameters are summarized in Table 1. We set the toroidal periodicity of the simulation domain $N_\alpha = 6$, and the half-widths of the ra-

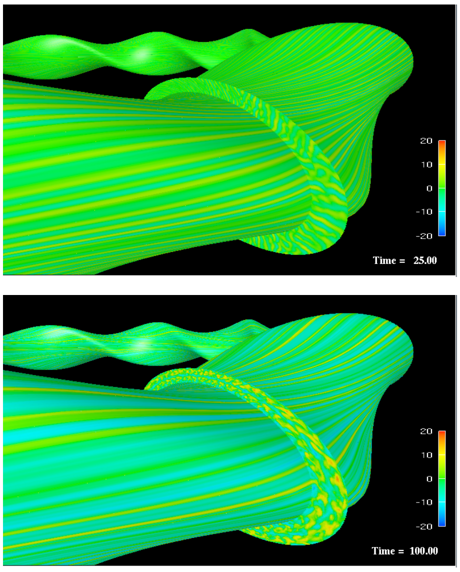

Fig. 2 Color contours of the electrostatic potential of the zonal flow and the ITG turbulence obtained by the GKV simulation for inward-shifted model configurations at t = 25 (upper) and $t = 100L_n/v_{ti}$ (lower).

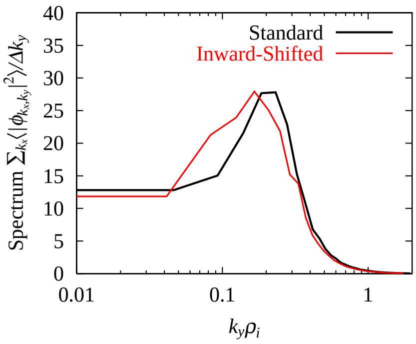

Fig. 3 Power spectra of potential fluctuations of the ITG turbulence obtained from the GKV simulations for the standard (black) and the inward-shifted (red) model configurations. The spectrum is time-averaged from t = 60 to $100L_n/v_{ti}$.

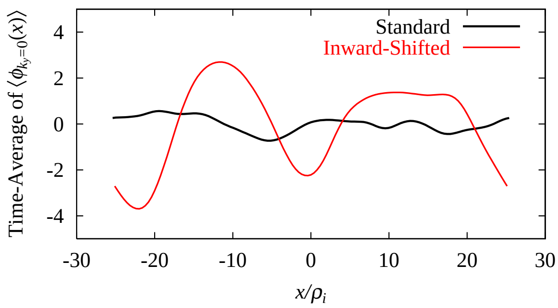

Fig. 4 Radial profiles of the zonal flow potential averaged from t = 60 to $250L_n/v_{ti}$. Black and red curves represent the results obtained from the standard and inward-shifted cases, respectively.

dial and toroidal (field-line-label) box size are given by $r_0\Delta q/q_0\hat{s}$ and $\pi r_0/q_0N_\alpha$, where the change of the safety factor $\Delta q = -1/6$.

Color contours of the electrostatic potential ϕ obtained from the GKV simulations of the ITG turbulence are shown in Figs. 1 and 2 for the standard and inward-shifted model configurations, respectively. Here, the potential fluctuations are mapped on the innermost flux surface and the elliptic poloidal cross-section. Radially-elongated eddy patterns of potential (streamers) are first driven by the toroidal ITG instability, and propagate in the direction of the ion diamagnetic drift. The ballooning-type mode structures are clearly found in the linear growth phase of the instability. The growth of the ITG instability is saturated by the self-generated $\boldsymbol{E}\times\boldsymbol{B}$ zonal flows, and the streamers are destroyed into small eddies in the later turbulent state.

Power spectra of the potential fluctuations of the ITG turbulence are shown in Fig. 3, where the data is time-averaged from t = 60 to $100L_n/v_{ti}$. We see the same peak amplitude of the spectrum, $\sum_{k_x}\langle|\phi_{k_x,k_y}|^2\rangle/\Delta k_y$ between the inward-shifted and standard cases, while the spectrum in the former broadens into the low-k_y side.

It is expected from the linear GKV simulations of the ITG mode [11] that, because of the higher maximum growth rate, ion thermal diffusivity, χ_i, grows faster for the inward-shifted configuration than for the standard one. In the nonlinear simulations, we have observed that the peak value of $\chi_i \simeq 3.8\rho_{ti}^2v_{ti}/L_n$ for the former case is about 50% larger than that of $\chi_i \simeq 2.6\rho_{ti}^2v_{ti}/L_n$ for the latter case. In the statistically steady states of the turbulent transport, however, χ_i averaged from t = 60 to $t = 250L_n/v_{ti}$ for the inward-shifted case is about 20% smaller than that from the result for the standard configurations, that is, $\chi_i \sim 1.45\rho_{ti}^2v_{ti}/L_n$ for the former case and $\chi_i \sim 1.78\rho_{ti}^2v_{ti}/L_n$ for the latter one. See also Ref. [17].

The lower ion heat transport found in the inward-shifted case is attributed to a larger amplitude of the zonal flows generated by turbulence. Radial profiles of the zonal flow potential are shown in Fig. 4, where the flux-surface average of the $k_y = 0$ components of the potential, $\langle\phi_{k_y=0}(x)\rangle$, are time-averaged from t = 60 to $t = 250L_n/v_{ti}$. The zonal-flow potential spectrum also shows about a three-times larger amplitude in the inward-shifted case than that in the standard configuration [17]. It should be noted that the stronger zonal-flow generation in the inward-shifted model configuration is consistent with larger values of the zonal-flow response function as discussed in our previous works [4, 5, 10, 11].

The transport reduction associated with the zonal-flow generation is also found in Lissajous plots of time-histories of the simulation data in Fig. 5, where the vertical axis measures the squared potential of the zonal flow, $\sum\langle|\phi_{k_x,0}|^2\rangle$. The horizontal axes in upper and lower panels

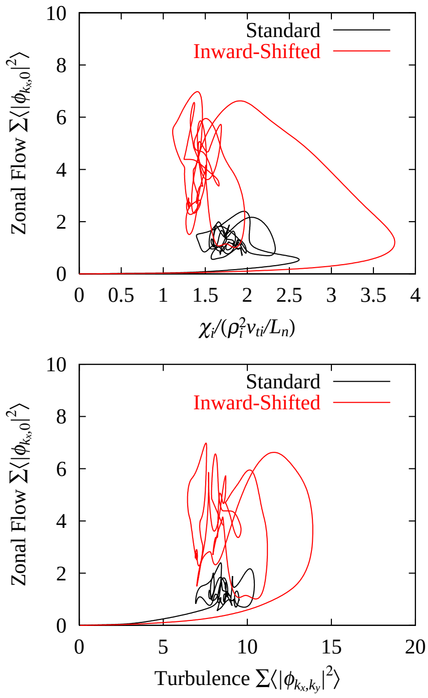

Fig. 5 Lissajous plots of the simulation results shown in the space of χ_i-$\sum\langle|\phi_{k_x,0}|^2\rangle$ (upper) and $\sum\langle|\phi_{k_x,k_y}|^2\rangle$- $\sum\langle|\phi_{k_x,0}|^2\rangle$ (lower). Black and red curves represent the results obtained from the standard and inward-shifted cases, respectively.

of Fig. 5 stand for the transport coefficient, $\chi_i/(\rho_{ti}^2 v_{ti}/L_n)$, and the turbulent fluctuations, $\sum\langle|\phi_{k_x,k_y}|^2\rangle$, respectively. In the upper panel, starting from the initial condition near the origin of $(0,0)$, the data point moves along the horizontal axis as the instability grows. One can see that χ_i is greatly reduced when the zonal flow is excited, where the orbit of the data point turns to the upper left corner of the figure. In the nonlinear saturation stage of the instability ($t > 60L_n/v_{ti}$), the data points for the two configurations fluctuate only inside two different regions, namely, the region with high transport and weak zonal flows for the standard configuration and the region with low transport and strong zonal flows for the inward-shifted configuration. Contrarily, the data points in the lower panel move around in a common horizontal range with a similar turbulent fluctuation level, but with different zonal flow amplitudes.

4 Conclusion

The nonlinear gyrokinetic-Vlasov simulations present the results that the ion thermal diffusivity χ_i driven by the ion temperature gradient turbulence for the inward-shifted LHD plasma takes a lower time-averaged value in the steady turbulent state because of the stronger zonal-flow generation. The obtained results confirm the theoretical prediction derived from the gyrokinetic analysis of the zonal flow response in helical systems, that is, the neoclassical optimization results in reduction of the anomalous transport through enhancement of the zonal flow. This provides ones a physical understanding on a possible mechanism of the confinement improvement found in the inward-shifted configurations of the LHD experiments.

Acknowledgments

This work is supported in part by grants-in-aid of the Ministry of Education, Culture, Sports, Science and Technology (No. 16560727, 17360445, and 17·05373), and in part by the National Institute for Fusion Science (NIFS) Collaborative Research Program (NIFS05KKMT001, NIFS06KTAT038, NIFS06KDAD006, and NIFS06KNXN060). Numerical simulations are carried out by use of the Earth Simulator under the support by Japan Agency for Marine-Earth Science and Technology, and by use of the Plasma Simulator and the LHD numerical analysis system at National Institute for Fusion Science.

[1] P.H. Diamond, S.-I. Itoh, K. Itoh, T.S. Hahm, Plasma Phys. Control. Fusion **47**, R35 (2005).

[2] N. Winsor, J.L. Johnson, J.J. Dawson, Phys. Plasmas **11**, 2448 (1968).

[3] R.M. Rosenbluth, F.L. Hinton, Phys. Rev. Lett. **80**, 724 (1998).

[4] H. Sugama and T.-H. Watanabe, Phys. Rev. Lett. **94**, 115001 (2005).

[5] H. Sugama and T.-H. Watanabe, Phys. Plasmas **13**, 012501 (2006).

[6] H.E. Mynick, Phys. Plasmas **13**, 058102 (2006).

[7] A. Fujisawa, et al., Phys. Rev. Lett. **93**, 165002 (2004).

[8] O. Motojima, et al., Nucl. Fusion **43**, 1674 (2003).

[9] H. Yamada, *et al.*, Plasma Phys. Controlled Fusion **43**, A55 (2001).

[10] T.-H. Watanabe, H. Sugama, and S. Ferrando-Margalet, Nucl. Fusion **47**, 1383 (2007).

[11] S. Ferrando-Margalet, H. Sugama, and T.-H. Watanabe, "*Zonal flows and ion temperature gradient instabilities in multiple-helicity magnetic fields*" Phys. Plasmas (2007) in press.

[12] T.-H. Watanabe, H. Sugama, Nucl. Fusion **46**, 24 (2006).

[13] O. Yamagishi, et al., Phys. Plasmas **14**, 012505 (2007).

[14] E.A. Frieman, L. Chen, Phys. Fluids **25**, 502 (1982).

[15] P.C. Clemmow, J.P. Dougherty, *Electrodynamics of Particles and Plasmas* (Addison-Wesley, Redwood City, 1969).

[16] M.A. Beer, S.C. Cowley, G.W. Hammett, Phys. Plasmas **2**, 2687 (1995).

[17] H. Sugama, T.-H. Watanabe, and S. Ferrando-Margalet, *Joint Conference of 17th International Toki Conference on Physics of Flows and Turbulence in Plasmas and 16th International Stellarator/Heliotron Workshop 2007* (Toki, Japan, 2007), I-08.